Supplemental Materials to ***Extraction of high-silica granites from an upper crustal magma reservoir: insights from the Narusongduo magmatic system, Gangdese arc*** by Jin-Sheng Zhou et al.

Supplemental materials contain in sequence:

Supplemental Analytical Methodology

Zircon U-Pb dating (LA-ICP-MS)

We took zircon separates from one andesite. Zircons were separated from bulk samples, using magnetic techniques and conventional heavy liquid. Representative zircon grains were handpicked under a binocular microscope, mounted in epoxy resin. Selected grains were photographed in transmitted, reflected light, and cathodoluminescence (CL) to examine the internal structure of zircons. Zircon U-Pb dating was conducted by a Finnegan Neptune multi-collector ICP-MS with a Newwave UP213 laser-ablation system at the Institute of Mineral Resources, Chinese Academy of Geological Sciences, Beijing. Detailed operating conditions for the instrument and analytical procedures are described by Hou et al (2009). Helium was utilized as the carrier gas to enhance the transport efficiency of the ablated material. All analyses were carried out with a beam diameter of 25 μm, repetition rate of 10 Hz, and energy of 2.5 J/cm^2. The masses ^{206}Pb, ^{207}Pb, ^{204}(Pb + Hg), and ^{202}Hg were determined by multi-ion-counters, and the masses ^{208}Pb, ^{232}Th, ^{235}U, and ^{238}U were collected by a Faraday cup. GJ-1 zircons were used as internal standards during the analyses. U, Th, and Pb concentrations were calibrated using the internal standard ^{29}Si and the external standard zircon M127 (U: 923 ppm; Th: 439 ppm; Th/U: 0.475; Nasdala et al., 2008). Off-line selection and integration of background and analytical signals, time-drift corrections and quantitative calibrations for the U–Pb dating were performed by the software ICPMSDataCal (Liu et al., 2010). Correction for common Pb was applied using the method of Andersen (2002).

Sr–Nd isotope analyses

Four whole-rock Sr and Nd isotopic compositions (sample NP3H-1, NP3H-7, NPII-18, and NPII-23) were performed by using a Finnegan Triton TI thermal ionization mass spectrometer at the State Key Laboratory for Mineral Deposit Research at Nanjing University, Nanjing, China. Detailed operating conditions for the instrument and analytical procedures are described by Pu et al (2005). The powders (200 mg for Sr–Nd isotope analyses) were leached in hot 6N twice sub-boiled HCl for 30 min. Samples were rinsed repeatedly (5–6 times) with milli-Q water, then ultrasonicated for 30 min to remove any residual traces of acid. After evaporation, all samples were dissolved for more than 36 h on a hotplate at approximately 130 ˚C with a mixture of HF-HNO_3 acids. Concentrated HNO_3 was added in samples to volatilize the residual HF, followed by additions of concentrated HCl and drying (repeat twice). The samples were dissolved in 4N HCl acid and Sr–Nd were separated from the matrix by chromatographic extraction using a cation exchange resin. The isotopic compositions were determined by a Finnigan MAT Triton TI thermal

ionization mass spectrometer. Sr and Nd ratios are normalized to $^{86}Sr/^{88}Sr$ = 0.1194, $^{146}Nd/^{144}Nd$ = 0.7219, respectively. Measured the La Jolla standard (recommended $^{143}Nd/^{144}Nd$ = 0.511850) and NBS-987 Sr standard (recommended $^{87}Sr/^{86}Sr$ = 0.710245) were 0.511842 ± 4 (2σ, n = 5) and 0.710260 ± 10 (2σ, n = 30), respectively. Total analytical blanks were less than 100 pg for Sr and Nd.

Cameca SXFiveFE electron microprobe analysis

Quantitative analyses of selected plagioclase profiles were performed on the Cameca SXFiveFE electron microprobe at Guangzhou Institute of Geochemistry, Chinese Academy of Sciences, with accelerating voltage of 20 kV, a beam current of 40 nA. A 3 μm beam diameter was employed for the analysis of the Mg profiles applied for calculation of melt composition. Magnesium was measured with peak counting times of 120 s, yielding a detection limit for Mg of 35–36 p.p.m. All analyses were calibrated using albite for Na; pyrope for Mg, olivine for Fe; orthoclase for K; $SrSO_4$ for Sr; plagioclase for Ca, Si, and Al; barite for Ba.

JEOL JXA-8800 electron microprobe analysis

Mineral compositions were determined using a JEOL JXA-8800 Superprobe at the Institute of Mineral Resources, Chinese Academy of Geological Sciences, Beijing, China. The microprobe was operated at an accelerating voltage of 15 kV, a beam current of 20 nA, and a beam size of 2-5 μm. These analyses were calibrated using jadeite (Si, Na, and Al), forsterite (Mg), orthoclase (K), apatite (P), wollastonite (Ca), rutile (Ti), and synthetic oxide (Cr, Mn, Fe, Ni) standards.

.

Modelling Methodology

Combined assimilation and fractional crystallization (AFC) modeling

The average andesitic composition is assumed as the parent melt. An assimilant composition is ancient crust-derived melts (represented by the ancient granites in the Gangdese arc, Zhang et al., 2012). Percentages of mineral phases were predicted by rhyolite-MELTS. Partition coefficients of Rb were obtained by $D_{Rb} = C_{Rb}^{mineral}/ C_{Rb}^{melt}$, where $C_{Rb}^{mineral}$ is the average content of Rb in minerals (determined by LA-ICP-MS) and C_{Rb}^{melt} is the average whole-rock content of Rb.

Rhyolite-MELTS modelling

Modelling of the liquid line of decent of the Narusongduo andesitic magmas were performed using the rhyolite-MELTS package (Gualda et al., 2012; Gualda and Ghiorso, 2015). The starting composition for modelling was based on the average whole-rock composition of the Narusongduo andesite with SiO_2 = 56.01wt%, TiO_2 = 0.89 wt%, Al_2O_3 = 17.24 wt%, Fe_2O_3 = 7.55 wt%, MnO = 0.13 wt%, MgO = 3.25 wt%, CaO = 6.38 wt%, Na_2O = 3.40 wt%, K_2O = 1.93 wt%, P_2O_5 = 0.22 wt%, and H_2O = 3 wt%. Initial water contents were estimated by the plagioclase-liquid hygrometer (Waters and Lang, 2015). Calcic plagioclases coexisting with clinopyroxene crystals were selected for estimation of initial magma water content and clinopyroxene P-T were input into plagioclase-liquid hygrometer. Redox conditions were set as ΔNNO = +1. Modelling was conducted at 220 MPa, using the average clinopyroxene pressure that was estimated by the clinopyroxene-liquid thermobarometer (Neave and Putirka, 2017). At these pressures rhyolite-MELTS predicts liquidus temperature of 1140.8 °C.

Rheology modelling

Changes in crystallinity, percentages of mineral phases, and residual liquid composition of the andesitic magmas were determined by the results from above Rhyolite-MELTS modeling. The viscosity of the liquids produced during subsequent crystallization were estimated using the method of Giordano et al. (2008). We evaluate the influence of increasing volume fraction of volatiles on liquid viscosity using the equation:

$$\log\eta_m = \log\eta_0 - \frac{\alpha \cdot \phi}{(1 - \phi)} \quad (1)$$

where η_m is the magma viscosity; η_0 is the viscosity of the melt phase calculated at each point; α is an adjustable fit parameter determined by experimental study and computed using a values of 2.5 from the literature in this study (Giordano et al., 2008). Rhyolite-MELTS modeling predicts the point of volatile saturation for the melt and increasing vol.% of the gas phase. The crystal volume fraction in magmas exceeds a critical value, causing a strong increase in viscosity and the onset of non-Newtonian behavior. Magma viscosities were calculated using the results for liquids together with the predicted amount of crystals from rhyolite-MELTS, using the methods outlined in Vona et al. (2011).

Plagioclase equilibrium liquid calculation

Plagioclase partition coefficients are dependent on An content and temperature (Blundy and Wood, 1991; Bindeman et al., 1998). The equations for plagioclase/silicate liquid partition coefficients (K) of Bindeman et al. (1998) were used to calculate the equilibrium liquid Mg contents, as follows:

$$RT \cdot \ln K = A_{\mathrm{Mg}} \cdot X_{\mathrm{An}} + B_{\mathrm{Mg}} \quad (2)$$

where A_{Mg} and B_{Mg} are empirically determined parameters; X_{An} the mole fraction of anorthite; R is the molar gas constant; T is the Kelvin temperature. The uncertainty in the calculated liquid Mg concentrations ($\sigma_{C_{liquid}}$) due to independent errors on the variables in Equation (2) was calculated by the error propagation formula:

$$\sigma_{C_{liquid}}^2 = \sigma_{C_{plagioclase}}^2 \left(\frac{\partial C_{liquid}}{\partial C_{plagioclase}}\right)^2 + \sigma_{A_{Mg}}^2 \left(\frac{\partial C_{liquid}}{\partial A_{Mg}}\right)^2 + \sigma_{B_{Mg}}^2 \left(\frac{\partial C_{liquid}}{\partial B_{Mg}}\right)^2 + \sigma_{X_{An}}^2 \left(\frac{\partial C_{liquid}}{\partial X_{An}}\right)^2 \quad (3)$$

where $\sigma_{A_{Mg}}$ and $\sigma_{B_{Mg}}$ are taken from Bindeman et al. (1998); $\sigma_{C_{plagioclase}}$ is errors in the measurement of plagioclase Mg contents from Cameca SXFiveFE electron microprobe analysis. The $\sigma_{X_{An}}$ is estimated by the formula:

$$\sigma_{X_{An}}^2 = \sigma_{C_{Ca}}^2 \left(\frac{\partial C_{X_{An}}}{\partial C_{Ca}}\right)^2 + \sigma_{C_{Na}}^2 \left(\frac{\partial C_{X_{An}}}{\partial C_{Na}}\right)^2 + \sigma_{C_K}^2 \left(\frac{\partial C_{X_{An}}}{\partial C_K}\right)^2 \quad (4)$$

where $\sigma_{C_{Ca}}$, $\sigma_{C_{Na}}$, and σ_{C_K} are errors in the measurements of plagioclase Ca, Na, and K contents from Cameca electron microprobe analysis.

Partition coefficients calculation

The lattice strain model was used for predicting the partition coefficients of REEs, Zr and Hf for clinopyroxene and amphibole (Blundy and Wood, 1994). According to the model, the partition coefficients of trace elements between mineral and liquid can be expressed as:

$$D_i^{Amp-liquid} = D_0 \exp\left[-\frac{4\pi E N_A}{RT}\left(\frac{r_0}{2}(r_0 - r_i)^2 - \frac{1}{3}(r_0 - r_i)^3\right)\right] \quad (5)$$

where D_i and D_0 are the theoretical and strain-free amphibole-liquid partition coefficients, respectively; r_0 is the optimum radius of the lattice site; r_i is the ionic radius of element; E is the effective Young's modulus; R is the gas constant (8.3145J/mol·K); N_A is Avogadro's number; T is Kelvin temperature. The parameters (D_0, r_0, E) are a function of pressure, temperature and composition, and were obtained by parameterized models based on mineral composition (Wood and Blundy, 1997; Hill et al., 2011; Shimizu et al., 2017).

Zr-saturation modeling

We assumed the average andesitic composition as the parent liquid and the initial melt Zr concentration equal to bulk rock. Residual liquid Zr content throughout the crystallization interval are calculated by bulk partition coeffcients for the saturated phases predicted by rhyolite-MELTS. Partition coefficients of Zr for plagioclase and amphibole were obtained by $D_{Zr} = C_{Zr}^{mineral} / C_{Zr}^{melt}$, where $C_{Zr}^{mineral}$ is the average content of Zr in minerals (determined by LA-ICP-MS) and C_{Zr}^{melt} is the average whole-rock content of Zr. Partition coefficients of Zr for

clinopyroxene were calculated by the lattice strain model (Blundy and Wood, 1994; Hill et al., 2011). The zircon solubility model of Boehnke et al. (2013) was employed to calculate the Zr concentration required for saturation in the evolving liquid.

Modeling of Zr/Hf ratio for the simultaneous crystallization of zircon and titanite

Numerical simulation of the effects on the Zr/Hf ratio of fractionated melts from the Narusongduo andesitic magmas. The effects of zircon were calculated by subtraction of Zr and Hf (Zr = 486400 ppm; Hf = 12720 ppm; calculated from a median composition of zircons (Wang et al., 2010). The effects of titanite were calculated with the Rayleigh fractionation equation ($C_l/C_0 = F^{D-1}$) for fractional crystallization ($K_d^{Zr} = 9.64$; $K_d^{Hf} = 18.7$; Bachmann et al., 2005).

Supplemental Figure

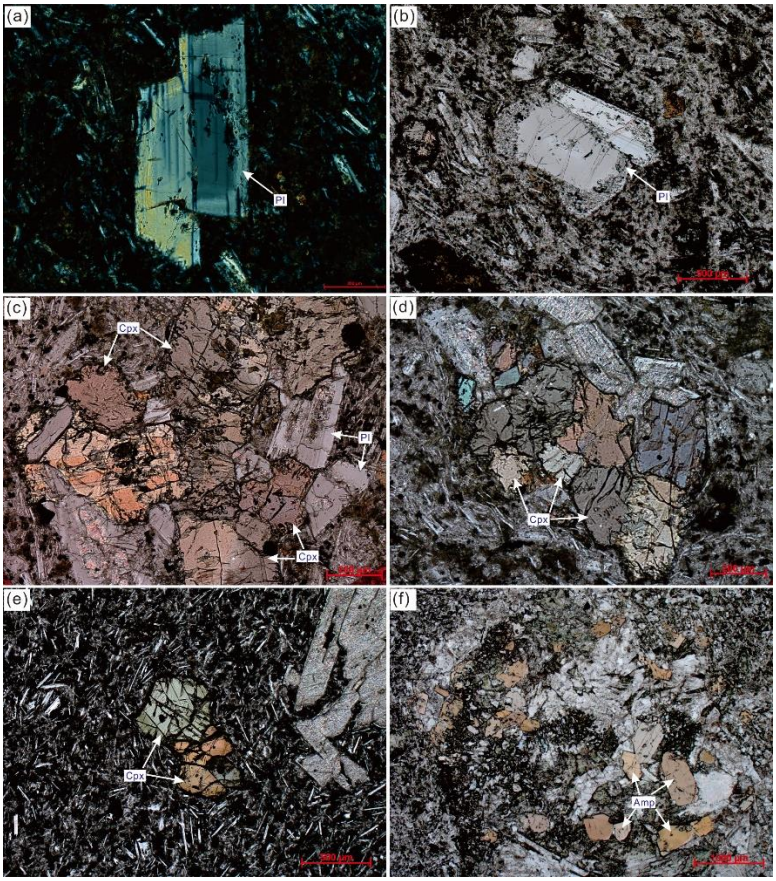

Figure S1. Photomicrographs showing petrographic features of the Narusongduo andesitic rocks. (a) Reversely zoned plagioclase. (b) Plagioclase crystal with sieve texture. (c) and (d) Glomerocrysts composed of clinopyroxene and plagioclase. (e) Discrete clinopyroxene phenocrysts. (f) Glomerocrysts composed of amphibole and quartz. Pl =

plagioclase; Cpx = clinopyroxene; Amp = amphibole.

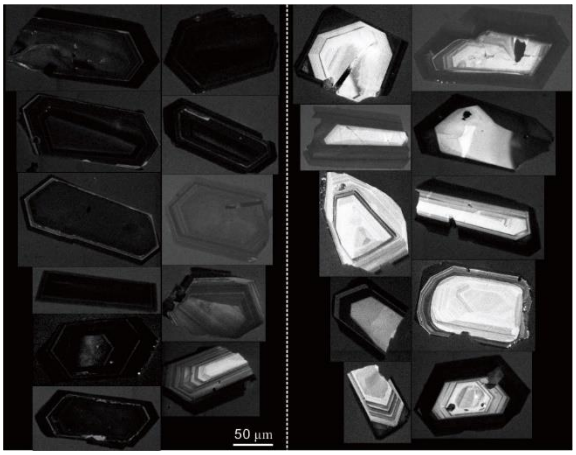

Figure S2. Cathodoluminescence (CL) images of representative zircon crystals from the HSGs. Zircon grains in the left and right halves are interpreted as autocrysts (dark) and antecrysts (bright), respectively.

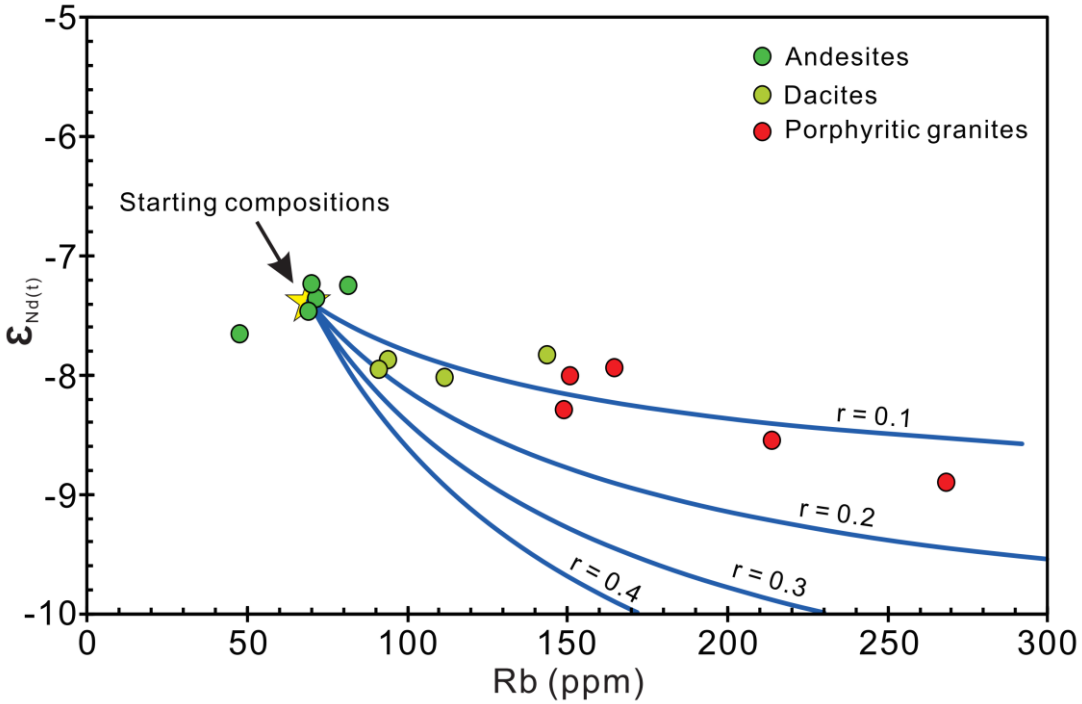

Figure S3. Whole-rock Rb contents vs $\varepsilon_{Nd(t)}$. AFC modeling of Nd isotopic data and Rb concentrations for the Naursongduo HSGs and dacites. The blue curves represent the combined assimilation and fractional crystallization (AFC) modeling results for different r values. The r value describes the ratio of assimilated material to crystallized material, and $r = m_a/m_c$, where m_a represents the mass fraction of assimilated material and m_c is the amount of crystallized material. Model parameters are listed in Supplemental Materials.

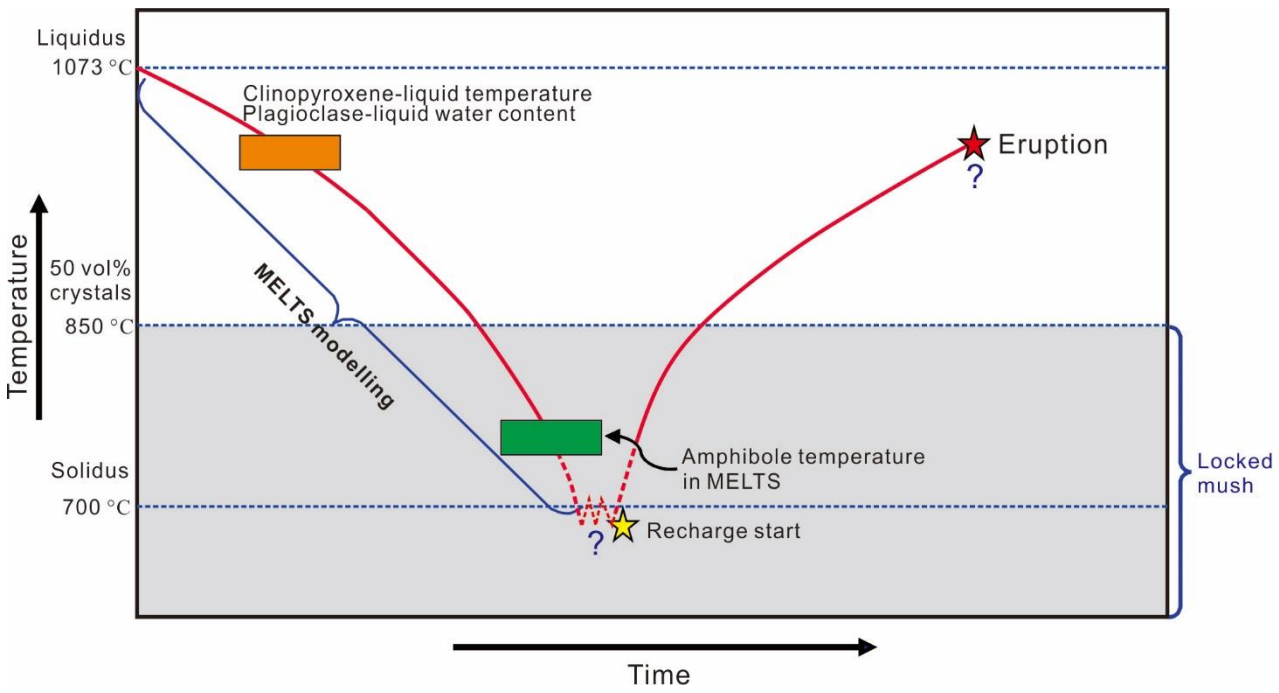

Figure S4. Schematic temperature-time diagram for the Narusongduo andesitic magma reservoir.

References

Andersen, T., 2002. Correction of common Pb in U–Pb analyses that do not report ^{204}Pb. Chemical Geology 192, 59–79. http://dx.doi.org/10.1016/S0009-2541(02)00195-X.

Bachmann, O., Dungan, M. A., Bussy, F., 2005. Insights into shallow magmatic processes in large silicic magma bodies: the trace element record in the Fish Canyon magma body, Colorado. Contrib. Mineral. Petrol. 149, 338-349. http://dx.doi.org/10.1007/s00410-005-0653-z.

Bindeman, I.N., Davis, A.M., Drake, M.J., 1998. Ion microprobe study of plagioclase-basalt partition experiments at natural concentration levels of trace elements. Geochim. Cosmochim. Acta 62, 1175–1193, https://doi.org/10.1016/S0016-7037(98)00047-7.

Blundy, J. D., Wood, B. J., 1991. Crystal-chemical controls on the partitioning of Sr and Ba between plagioclase feldspar, silicate melts, and hydrothermal solutions. Geochim. Cosmochim. Acta 55, 193-209, https://doi.org/10.1016/0016-7037(91)90411-W.

Blundy, J., Wood, B., 1994. Prediction of crystal–melt partition coefficients from elastic moduli. Nature 372, 452-454. https://doi.org/10.1038/372452a0.

Boehnke, P., Watson, E. B., Trail, D., Harrison, T. M., Schmitt, A. K., 2013. Zircon saturation re-revisited. Chem. Geol. 351, 324-334. http://dx.doi.org/10.1016/j.chemgeo.2013.05.028.

Giordano, D., Russell, J. K., Dingwell, D. B., 2008. Viscosity of magmatic liquids: a model. Earth Planet. Sci. Lett. 271, 123-134, https://doi.org/10.1016/j.epsl.2008.03.038.

Gualda, G. A., Ghiorso, M. S., 2015. MELTS_Excel: A Microsoft Excel-based MELTS interface for research and teaching of magma properties and evolution. Geochem. Geophys. Geosyst. 16, 315-324. https://doi.org/10.1002/2014GC005545.

Gualda, G.A.R., Ghiorso, M.S., Lemons, R.V., Carley, T.L., 2012. Rhyolite-MELTS: A modifed calibration of MELTS optimized for silica-rich, fluid-bearing magmatic systems. J. Petrol. 53, 875–890. https://doi.org/10.1093/petrology/egr080.

Hill, E., Blundy, J. D., Wood, B. J., 2011. Clinopyroxene–melt trace element partitioning and the development of a predictive model for HFSE and Sc. Contrib. Mineral. Petrol. 161, 423-438. https://doi.org/10.1007/s00410-010-0540-0.

Hou, K. J., Li, Y. H., Tian, Y. Y., 2009. In situ U–Pb zircon dating using Laser Ablation Multi Ion Counting-ICP-MS. Mineral Deposits 28, 481–492[in Chinese with English abstract].

Ji, X. H., Yang, Z. S., Yu, Y. S., Shen, J. F., Tian, S. H., Meng, X. J., Li, Z. Q., Liu, Y. C., 2012. Formation mechanism of magmatic rocks in Narusongduo lead-zinc deposit of Tibet: Evidence from magmatic zircon. Mineral Deposits 31, 758-774 [in Chinese with English abstract].

Liu, Y., Gao, S., Hu, Z., Gao, C., Zong, K., Wang, D., 2010. Continental and oceanic crust recycling-induced melt-peridotite interactions in the Trans-North China orogen: U–Pb dating, Hf isotopes and trace elements in zircons of mantle xenoliths. J. Petrol. 51, 537–571. http://dx.doi.org/10.1093/petrology/egp082.

Nasdala, L., Hofmeister, W., Norberg, N., Mattinson, J.M., Corfu, F., Dörr, W., Kamo, S.L., Kennedy, A.K., Kronz, A., Reiners, P.W., Frei, D., Kosler, J., Wan, Y., Götze, J., Häger, T., Kröner, A., Valley, J.W., 2008. Zircon M257—a homogeneous natural reference material for the ion microprobe U–Pb analysis of zircon. Geostand. Geoanal. Res. 32, 247–265. http://dx.doi.org/10.1111/j.1751-908X.2008.00914.x.

Neave, D. A., Putirka, K. D., 2017. A new clinopyroxene-liquid barometer, and implications for magma storage pressures under Icelandic rift zones. Am. Mineral. 102, 777-794. http://dx.doi.org/10.2138/am-2017-5968.

Pu, W., Gao, J. F., Zhao, K. D., Ling, H. F., Jiang, S. Y., 2005. Separation method of Rb-Sr, Sm-Nd using DCTA and HIBA. J. Nanjing Univ. (Nat. Sci.) 41: 445–450 [in Chinese with English abstract].

Shimizu, K., Liang, Y., Sun, C., Jackson, C. R., Saal, A. E., 2017. Parameterized lattice strain models for REE partitioning between amphibole and silicate melt. Am. Mineral. 102, 2254-2267. https://doi.org/10.2138/am-2017-6110.

Vona, A., Romano, C., Dingwell, D. B., Giordano, D., 2011. The rheology of crystal-bearing basaltic magmas from Stromboli and Etna. Geochim. Cosmochim. Acta 75, 3214-3236. https://doi.org/ 10.1016/j.gca.2011.03.031.

Wang, X., Griffin, W. L., Chen, J., 2010. Hf contents and Zr/Hf ratios in granitic zircons. Geochem. J. 44, 65-72. http://dx.doi.org/10.2343/geochemj.1.0043.

Waters, L. E., Lange, R. A., 2015. An updated calibration of the plagioclase-liquid hygrometer-thermometer applicable to basalts through rhyolites. Am. Mineral. 100, 2172-2184. https://doi.org/10.2138/am-2015-5232.

Wood, B. J., Blundy, J. D., 1997. A predictive model for rare earth element partitioning between clinopyroxene and anhydrous silicate melt. Contrib. Mineral. Petrol. 129, 166-181. https://doi.org/10.1007/s004100050330.

Zhang, X.Q., Zhu, D.C., Zhao, Z.D., Sui, Q.L., Wang, Q., Yuan, S.H., Hu, Z.C., Mo, X.X., 2012. Geochemistry, zircon U-Pb geochronology and in-situ Hf isotope of the Maiga batholith in Coqen, Tibet: constraints on the petrogenesis of the Early Cretaceous granitoids in the central Lhasa Terrane. Acta Petrol. Sin. 28, 1615–1634 [in Chinese with English abstract].